

Development of a 3D Tissue-Engineered Skeletal Muscle and Bone Co-culture System

Nicholas M. Wragg,* Diogo Mosqueira, Lia Blokpeol-Ferreras, Andrew Capel, Darren J. Player, Neil R. W. Martin, Yang Liu, and Mark P. Lewis

In vitro 3D tissue-engineered (TE) structures have been shown to better represent in vivo tissue morphology and biochemical pathways than monolayer culture, and are less ethically questionable than animal models. However, to create systems with even greater relevance, multiple integrated tissue systems should be recreated in vitro. In the present study, the effects and conditions most suitable for the co-culture of TE skeletal muscle and bone are investigated. High-glucose Dulbecco's modified Eagle medium (HG-DMEM) supplemented with 20% fetal bovine serum followed by HG-DMEM with 2% horse serum is found to enable proliferation of both C2C12 muscle precursor cells and TE85 human osteosarcoma cells, fusion of C2C12s into myotubes, as well as an upregulation of RUNX2/CBFA1 in TE85s. Myotube formation is also evident within indirect contact monolayer cultures. Finally, in 3D co-cultures, TE85 collagen/hydroxyapatite constructs have significantly greater expression of RUNX2/CBFA1 and osteocalcin/BGLAP in the presence of collagen-based C2C12 skeletal muscle constructs; however, fusion within these constructs appears reduced. This work demonstrates the first report of the simultaneous co-culture and differentiation of 3D TE skeletal muscle and bone, and represents a significant step toward a full in vitro 3D musculoskeletal junction model.

1. Introduction

Currently, in vitro biotoxicity testing of developmental pharmaceuticals, biomaterials, and medical devices is performed on in vitro monolayer cell culture models (ISO10993). Monolayer models are capable of identifying cytotoxic effects through morphological and biochemical assays or by assessing changes in gene expression.^[1] However, these results do not effectively translate across to in vivo tissue systems.^[1,2] This is due to a general failure to accurately recapitulate the complex nature of native tissue structures and the biochemical pathways that accompany such architecture, therefore justifying the use of animal models.^[3–6] Animal models clearly demonstrate complex tissue structures and pathways, although these models have accompanying high costs, contentious ethical considerations, and results that do not always translate across species.^[7,8] As such, there is a growing need for more complex in vitro models, which provide more representative

structures and physiology than conventional cell cultures, without the complexities of animal research.


Development of increasingly relevant models has shown the potential of 3D tissue-engineered (TE) solutions for in vitro pre-clinical testing.^[2,9–12] Engineered constructs require a cell source capable of forming the structures and processes associated with in vivo tissues. This is in addition to environmental conditions, such as a substrate/scaffold and specific nutrients, which enable the establishment of these characteristics. However, due to the very different physical structures of each of these tissues and hence their culture conditions, in vitro 3D models of skeletal muscle and bone have yet to be cultured together.

Myogenic differentiation in both monolayer and 3D requires muscle progenitor cells (MPCs), or myoblasts, to exit the cell cycle. In vitro, this is generally met through a reduction in serum content to induce cellular fusion.^[13–17] Current 3D muscle models use this process in tandem with a scaffold to act as an extracellular matrix. This is typically a cell-seeded hydrogel, which is tethered during the setting of the hydrogel or during the culture, as MPCs delaminate and self-assemble between the anchor points.^[18–25] MPCs align according to lines of isometric tension, which are formed through cell-mediated scaffold contraction over the culture period.^[26] This helps to create highly aligned popula-

Dr. N. M. Wragg, Dr. D. Mosqueira, Dr. L. Blokpeol-Ferreras, Dr. A. Capel, Dr. D. J. Player, Dr. N. R. W. Martin, Prof. M. P. Lewis
School of Sport, Exercise and Health Sciences
Loughborough University
Loughborough, UK
E-mail: n.m.wragg2@lboro.ac.uk

Dr. N. M. Wragg, Dr. Y. Liu
Wolfson School of Mechanical
Electrical and Manufacturing Engineering
Loughborough University
Loughborough, UK

Dr. D. J. Player
Institute of Orthopaedics and Musculoskeletal Sciences
RNOH University College London
Stanmore, UK

 The ORCID identification number(s) for the author(s) of this article can be found under <https://doi.org/10.1002/biot.201900106>

© 2019 The Authors. *Biotechnology Journal* published by WILEY-VCH Verlag GmbH & Co. KGaA, Weinheim. This is an open access article under the terms of the Creative Commons Attribution License, which permits use, distribution and reproduction in any medium, provided the original work is properly cited.

DOI: 10.1002/biot.201900106

tions of myotubes, which better represents in vivo structure than monolayer cultures.^[5]

TE bone models also utilize a scaffold and either an osteoblast-like cell line or a multipotent stem cell, for example a mesenchymal stem cell, to act as a source of matrix deposition and remodeling.^[27–29] There are many different types of bone scaffold based on synthetic or naturally derived materials.^[30–36] Individually, each of these scaffold types have disadvantages, such as reduced cell affinity.^[28,37] However, by combining materials to create a hybrid/composite scaffold, these disadvantages can be reduced or eradicated to assist in the formation of a more relevant bone-like model.^[38–41] The addition of ascorbic acid, β -glycerophosphate, and dexamethasone have been shown to increase RUNX2/CBFA1 expression and matrix production, as well as the formation of bone mineral in osteoblast/osteoblast-like cells.^[42]

By comparing the effects of reported skeletal muscle and bone medium compositions on both cell populations in monolayer and 3D, this work sought to establish conditions conducive to the co-culture of 3D TE skeletal muscle and bone toward the formation of an in vitro musculoskeletal junction (muscle–tendon–bone). This would greatly increase the physiological relevance of in vitro toxicology testing before in vivo studies and could aid in the understanding of musculoskeletal diseases.

2. Experimental Section

2.1. Cell Culture

Cell populations were cultured under humidified atmospheric O₂ and 5% CO₂ conditions at 37 °C (5% CO₂ in air). Medium compositions were based upon previous literature (Table 1).^[16,43–46] C2C12 murine MPCs (ECACC, UK) were expanded in M1. All experiments were conducted prior to passage 8. TE85 human osteosarcoma (hOS) cells (ATCC, UK), were expanded in M2, or growth medium (GM) as detailed for C2C12s (M1). All experiments were conducted prior to passage 60.

2.2. Media Composition Culture Comparisons

2.2.1. Proliferation Phase

Both cell lines were seeded at 4500 cells cm⁻² in six-well plates and cultured for 4 days in M1, M2, or M3. Cells were lysed and processed for DNA and protein analysis at 24, 48, and 96 h postseeding. Metabolic activity was measured at 96 h, and then samples were passaged for live cell number and membrane integrity (viability). Brightfield micrographs were taken using a Leica DMIL LED light microscope prior to lysis for morphological analysis.

2.2.2. Differentiation Phase

Based on results of the proliferation phase cell culture, a single maintenance medium (M1) was chosen to culture the cells prior to differentiating. Cells were cultured as detailed during the proliferation phase. Once confluent, cells were cultured in either osteogenic or myogenic differentiation media for 3 days. M2 was

Table 1. Medium compositions.

Growth medium designation	Components
M1—Skeletal muscle precursor maintenance medium	<ul style="list-style-type: none"> – Dulbecco's modified Eagle media (DMEM)—High glucose (Hyclone) – 20% Fetal bovine serum (FBS) (PAN Biotech) – 1% Penicillin/streptomycin (PS) (10 000U mL⁻¹ and 10 000 μg mL⁻¹; Gibco)
M2—Human osteosarcoma maintenance medium	<ul style="list-style-type: none"> – Eagle's minimum essential medium (EMEM)—Earle's balanced salt solution (EBSS) (Sigma) – 10% FBS – 1% L-Glutamine (200 mM; Sigma) – 1% Non-essential amino acids (NEAA) (100\times; Sigma) – 1% PS
M3—Osteoblast-like cell maintenance medium	<ul style="list-style-type: none"> – DMEM—low glucose (Sigma) – 10% FBS – 1% PS
MM—Myogenic medium	<ul style="list-style-type: none"> – DMEM (high glucose) – 2% Horse serum – 1% PS
OM—Osteogenic medium	<ul style="list-style-type: none"> – DMEM (low glucose) – 10% FBS – 0.1 μM Dexamethasone (Sigma) – 0.05 mM Ascorbic acid (Sigma) – 10 mM β-Glycerol-phosphate (Sigma) – 1% L-Glutamine – 1% PS

used as a control for the TE85s. Cells were lysed for analysis at 24, 48, and 72 h postseeding.

2.3. Indirect Contact Co-culture of C2C12 MPCs and TE85 hOS

Polydimethylsiloxane (PDMS, Sylgard 184 Elastomer) was pre-set in six-well plates (Nunc) and cut to provide a central barrier approximately 0.5 \times 3.5 \times 0.5 mm across the wells (Figure 1). C2C12 MPCs and TE85 hOS cells were seeded separately at 4500 cells cm⁻² in 2.0 mL of GM (M1) either side of the barrier and left to attach for 2 h. GM (M1) was added to each well until the levels rose above the PDMS (ca. 6.0 mL) and 2.0 mL replenished daily. At confluency (ca. 72 h postseeding), GM was removed and replaced with 1.0 mL myogenic medium (MM) and 0.32 mg mL⁻¹ hydroxyapatite (HA) in MM to the C2C12s and TE85s, respectively. Cultures were left for 2 h at 37 °C/5% CO₂ in air to allow the HA to settle onto the TE85s. MM was then gently added to the well on top of the boundary to increase levels above the PDMS barrier (ca. 6.0 mL). Cells were lysed for analysis after 3 days. Controls of MPC/hOS – HA, hOS – HA/hOS – HA, MPC/MPC, hOS + HA/hOS + HA, and MPC/MPC with HA conditioned medium were set up simultaneously.

2.4. TE 3D Collagen Constructs

2.4.1. Skeletal Muscle Model

Skeletal muscle constructs were prepared according to an adjusted protocol.^[5,16] Briefly, 10 \times minimal essential medium (MEM) (Gibco) was added to 2.0 mg mL⁻¹ type-1 rat tail collagen

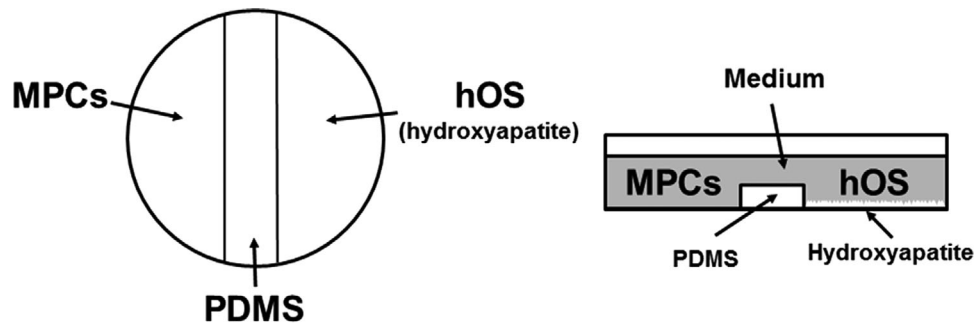


Figure 1. Monolayer co-culture systems. Each cell type was separated by a PDMS boundary with secreted and degradation products shared within the medium. Both cell types exposed to a single medium by filling the well to a volume above the height of the boundary.

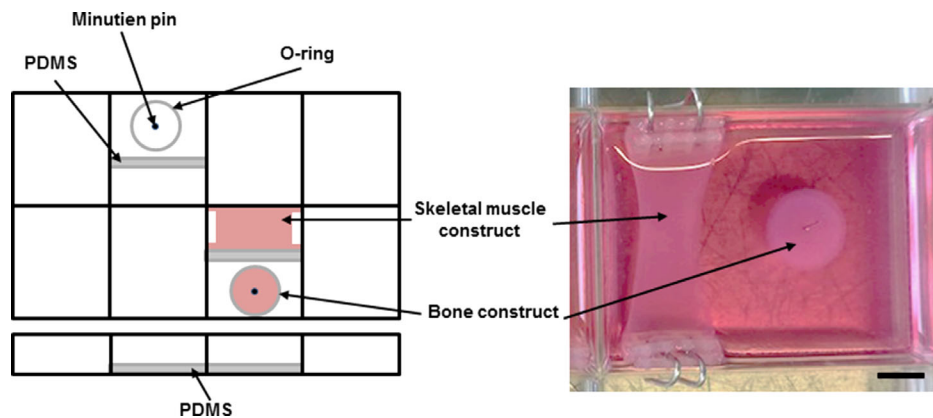


Figure 2. Schematic of 3D tissue-engineered co-culture system. (Left) To create the bone construct setting area, the threaded section of a 15-mL centrifuge tube was removed and placed on a PDMS-coated well. The ring was then sealed to the PDMS with 2.0 mg mL^{-1} collagen. A Minutien pin was placed in the center of the ring to act as an anchor point for the bone construct. A PDMS boundary was placed adjacent to the ring and sealed with collagen. Not to scale. (Right) 3D skeletal muscle and bone constructs after 14 days culture. Scale bar = 5 mm.

(First Link, UK) and mixed thoroughly. This solution was then neutralized using 5 M and 1 M NaOH until a color change from yellow to pink was observed. MPCs suspended in GM (M1) were then added to the collagen solution and pipetted into a defined setting area (15 mm x 28 mm) with bespoke anchor points, termed “A-frames” at either end (Figure 2). The final solution comprised 85% collagen, 10% 10× MEM, and 5% cell suspension. Each A-frame consists of poly(ethylene-co-1-octene) plastic 10 count canvas mesh (Darice) bound together with 0.3 mm stainless steel wire (Scientific Wire Company, UK) to form a floatation bar. Note that 0.3 mm wire was used to create a hook, which could be pushed into the floatation bar and hung over the side of the setting chamber to keep the construct stable.

2.4.2. Bone Model

HA solution and collagen/HA 3D constructs were prepared according to an adjusted protocol.^[47]

Hydroxyapatite solution preparation: Note that 500 mL of 130 mM analytical grade ammonium phosphate tribasic trihydrate (NBS Biologicals Ltd) was added dropwise into 500 mL of 210 mM calcium acetate solution. The solution was continuously stirred and maintained at pH12 and 3 °C by adding concentrated ammonium hydroxide and housing in a bath of iced water. The

precipitate solution was then placed into a refrigerator at 4 °C and left to age overnight. During the aging process, the precipitate settles creating a clear phase separation. The HA precipitate was washed periodically in dH_2O while in storage to retain phase separation. Samples of the HA suspension were then aliquoted into 50 mL tubes (FisherBrand) and centrifuged at 4000 rpm for 5 min. The clear phase was removed and replaced with dH_2O . After resuspension in dH_2O , 3.7% hydrochloric acid (HCl) was added to adjust the pH to 7.5, followed by a final wash in dH_2O . Once neutralized, the centrifugation process was repeated until unbound water was negligible, creating a concentrated HA paste. The concentration of HA in the paste was measured by calculating the dry mass as a percentage of the initial sample mass. The dry mass was obtained by measuring a sample after baking at 80 °C for 30 min.

Bone collagen/hydroxyapatite model: HA was added to 2.0 mg mL^{-1} type-1 rat tail collagen in 0.1 M acetic acid (First Link, UK) to the required concentration and mixed thoroughly. 10× MEM (Gibco) was added to this mixture and then neutralized using 5 M and 1 M NaOH until a color change from yellow to pink was observed. TE85 hOS cells suspended in M1 were then added to the collagen solution and pipetted into a bespoke plastic O-ring (ca. 16 mm internal diameter). The final solution comprised 85% collagen/HA solution, 10% 10× MEM, and 5% cell suspension.

Table 2. Quantitative reverse transcription PCR (qRT-PCR) primers.

Target mRNA (M—mouse; H—human)	Primer sequences 5'–3'		Reference sequence accession number
	Forward	Reverse	
POLR2B (M)	GGTCAGAAGGGAAGTGTGGTAT	GCATCATAAATGGAGTAGCGTC	NM_153798.2
POLR2B (H)	AAGGCTTGGTTAGACAACAG	TATCGTGCCGGTCTTCA	NM_000938.1
Myogenin (M)	CCAACTGAGATTGTCTGTC	GGTGTAGCCTTATGTGAAT	NM_031189.2
RUNX2/CBFA1 (H/M)	GCAGTATTACAACAGAGGG	TCCCAAAAGAAGTTTTGCTG	NM_001145920
Osteocalcin/BGLAP(H)	CTCACACTCCTGCCCTATT	TCCCAGCCATTGATACAGGT	NM_199173

2.5. Co-culture Platform for 3D TE Skeletal Muscle and Bone Constructs

3D co-culture molds were created using Nunc Rectangular 8-well plates coated with PDMS. An area large enough to allow for the setting of the skeletal muscle construct and placement of the boundary was cut away from the PDMS covering the well, and a bespoke plastic O-ring was placed onto the remaining PDMS covering the well. Note that 2.0 mg mL⁻¹ collagen was used to seal the resulting ring to the PDMS creating a well to set the bone construct in. A minutien pin was placed at the center to act as an anchor point for the bone construct. A separate PDMS boundary was used to create the setting area for the skeletal muscle construct and sealed using 2.0 mg mL⁻¹ collagen (Figure 2).

Once the skeletal muscle and collagen/cell solutions were pipetted into the setting areas, the chamber was placed into a 37 °C humidified incubator and left until the collagen mixtures were fully polymerized. Once set, the construct was detached from the walls of the setting area, the PDMS and O-ring boundary wall were removed, and M1 was added to the well, allowing the construct to float. Constructs were cultured for 4 days in M1, ensuring complete replacement of the medium twice daily. To induce cellular fusion, constructs were then cultured in MM for a further 10 days, ensuring complete replacement of MM every 24 h.

2.6. Cyto- and Histochemistry

Fluorescent cell staining was performed as follows. Numbers in brackets represent timings used when working with 3D collagen scaffolds to enable liquid penetration through the matrix.

Following culture, the cells were washed twice with phosphate-buffered saline (PBS) and fixed by the dropwise addition of methanol and acetone (1:1 v/v) to PBS (50% v/v). This was removed after 15 (30) min incubation, and neat methanol and acetone (1:1 v/v) was added for a further 15 (30) min prior to staining.

Once fixed, cultures were stained for the muscle-specific cytoskeletal intermediate filament desmin. Initially constructs were placed into a blocking solution consisting of 5% goat serum and 0.2% Triton X-100 in Tris-buffered saline (TBS) for 30 min (2 h) and then incubated with rabbit anti-desmin antibody (Abcam, UK) for 2 h (overnight) diluted 1:200 in 2% goat serum/TBS. The cells were then incubated in the dark for a further 2 h in goat anti-rabbit IgG rhodamine-derived tetramethylrhodamine (TRITC) or Chromeo 488 conjugated secondary

antibody (Abcam) diluted 1:200 in TBS. For indirect contact monolayer cultures, phalloidin conjugated with the fluorescent dye rhodamine was used to visualize cytoskeletal F-actin (Life Technologies). Samples were incubated in a 1:200 solution of rhodamine phalloidin with 0.1% Triton-X in PBS for 30 min.

DAPI was used as a counterstain to observe cell nuclei. Samples were incubated in a 1:10 000 dilution (1 mg mL⁻¹; Thermo Scientific Pierce) in dH₂O for 15 (30) min in the dark before being washed at least five times in dH₂O. All samples were mounted on glass microscope slides using Fluoromount Aqueous Mounting Medium (Sigma) and imaged using a Leica DM2500 fluorescence microscope with associated software.

2.7. RNA Extraction and Quantitative RT-PCR

Monolayer samples used for quantitative RT-PCR (qRT-PCR) analysis were first lysed in 500 µL TRI-reagent (Fisher). 3D cultures were placed into 500 µL TRI reagent and snap frozen in liquid nitrogen. Samples were then stored at –80 °C for later RNA extraction.

Prior to RNA extraction, samples were thawed at room temperature. A steel ball bearing was added to 3D construct samples and then agitated on a TissueLyser II (Qiagen) for 4 min at 10 000 rpm to ensure homogenization and cell lysis. RNA was extracted using TRI-Reagent (Sigma) according to manufacturer's guidelines. qRT-PCR reactions were performed using QuantiFast SYBR Green RT-PCR kit (Qiagen) and primers (Table 2) with cycling as follows: 50 °C for 10 min (reverse transcription/cDNA synthesis), 95 °C for 5 min (transcriptase inactivation and initial denaturation step) followed by PCR steps for 40 cycles; 95 °C for 10 s (denaturation), 60 °C for 30 s (annealing and elongation). Finally, a dissociation/melt curve analysis was performed to allow exclusion of nonspecific amplification or primer–dimer interference. Relative gene expression was calculated using $\Delta\Delta\text{CT}$ equation^[48] where relative expression is calculated as $2^{-\Delta\Delta\text{CT}}$ (fold change). Each individual sample was assessed in triplicate and normalized to a single designated POLR2B reference gene.

2.8. Alkaline Phosphatase Activity, DNA, and Protein Quantification

Monolayer samples taken for alkaline phosphatase (ALP), DNA, and protein analysis were lysed in dH₂O and taken through three

freeze-thaw cycles. 3D TE samples were snap frozen with 500 μL of dH_2O in liquid nitrogen. Samples were stored at -80°C for later use. A steel ball bearing was added to 3D construct samples and then agitated on a TissueLyser II (Qiagen) for 4 min at 10 000 rpm. For studies not involving direct contact with HA, DNA content was measured using a NanoDrop 2000 spectrophotometer at 260 nm (Thermo Scientific). For studies involving direct contact with HA, commercially available Quant-iT PicoGreen dsDNA Kits (Invitrogen) were used according to manufacturer's guidelines.

ALP was measured using a 4-methylumbelliferyl phosphate (MUP) dephosphorylation assay in which 50 μL of the cell/lysis buffer solution was placed into a 96-well plate with 50 μL of dH_2O . To this, 50 μL of 4-MUP was added and left for 30 min. To stop the reaction, 50 μL of 100 mM EDTA buffer was added. Absorbance readings taken using a Varioskan Flash (ThermoScientific) at 440 nm. Results were compared with a standard curve of 4-MU. ALP was normalized to DNA for later construct configuration comparison. Protein concentrations were measured using a NanoDrop 2000 spectrophotometer at 280 nm.^[49]

2.9. Metabolic Activity per Live Cell and Membrane Integrity Measurements

Metabolic activity was measured using a 10% (v/v) solution of PrestoBlue (Invitrogen) in the respective GM. Cells were incubated for 30 min in culture conditions and then 100 μL sampled and read at 544 nm/590 nm (excitation/emission) using a Varioskan Flash. Following trypsinization, membrane integrity (viability) and live cell numbers were measured using an Acridine Orange (30 $\mu\text{g mL}^{-1}$)/DAPI (100 $\mu\text{g mL}^{-1}$) solution and image analysis on Nucleocounter NC-3000 (Chemometec).

2.10. Myotube Characteristics

Mean number of myotubes, fusion index (percentage of nuclei attributed to myotubes), and mean number of nuclei per myotube were measured manually from fluorescent images using ImageJ (NIH).

2.11. Statistics

All data are presented as mean \pm standard deviation. To determine if statistical differences existed between different medium compositions or indirect co-cultures, analyses of variance (ANOVA) were performed with a Bonferroni post hoc test. The results of the 3D TE co-cultures were analyzed using a two-tailed *t*-test. All statistical analyses were conducted using GraphPad Prism 5.0.

3. Results

3.1. Medium Composition Culture Comparisons

To create a system in which the major musculoskeletal components of skeletal muscle and bone can be co-cultured in

3D, a medium must first be identified that can sustain the growth and differentiation of both cell types. Three proliferation phase media were tested, followed by differentiation phase analysis using a myogenic and an osteogenic medium (Table 1). DNA concentration changes were used as an indicator of population change and protein/DNA ratios as an indicator of cell size.

3.1.1. Proliferation Phase

After 48 h, both C2C12 and TE85 DNA and protein (Figure 3A–D) concentrations increased without any significant differences occurring between the three growth media. After 96 h, C2C12s grown in M1 (C2C12 control medium) had significantly greater DNA and protein concentrations than those cultured in M2 and M3 ($p \leq 0.001$), demonstrating greater proliferation in this control media. Contrastingly, TE85s cultured in M2 (TE85 control medium) had significantly greater DNA and protein concentrations than either M1 or M3 at 96 h ($p \leq 0.001$). TE85s cultured in M3 exhibited reduced concentrations of DNA and protein compared to both M1 and M2, respectively; therefore, to achieve a consistent proliferation timeline comparative to previous cultures and models, M3 would be unsuitable for co-culture. These trends can also be observed in brightfield images (Figure S1, Supporting Information) with increasing coverage to full confluency for all conditions after 96 h, except for TE85s cultured in M3, which show large areas of uncovered surface. Protein/DNA (Figure 3E,F) ratios indicate changes in cellular population morphology. After 96 h, no significant differences occur between M1, M2, or M3 conditions in both C2C12 and TE85 cultures.

These data indicate that each medium condition produced only a proliferative effect rather than additional changes in cell size (hyperplasia rather than hypo- or hypertrophy), although a numerical bias toward the control media was observed. This bias was more pronounced without a preconditioning step, where changes in basal medium (from DMEM to EMEM or EMEM to DMEM) resulted in significantly less ($p < 0.001$) DNA concentrations at 96 h after seeding (Figure S1, Supporting Information).

Additionally, for C2C12s cultured in M1, metabolic activity per live cell (MAC) was slightly greater, although not statistically significant (Figure 3G,H). Conversely, for TE85s, M1 cultures exhibited a slightly lower nonsignificant MAC, potentially reflecting the lower 96-h DNA profile than M2 culture despite nonsignificance after 48 h. Membrane integrity (Figure 3 I,J), following passage at 96 h, was not significantly different in C2C12s (ca. 93%). In TE85 M1 cultures, membrane integrity was statistically significantly lower, although this difference is considered negligible (ca. $96.0 \pm 1.0\%$ vs ca. $98.0 \pm 0.4\%$).

Although TE85s cultured in M2 demonstrated significantly greater DNA concentrations after 96 h, TE85 M1 cultures were still able to reach full confluency, while M2 affected C2C12 cultures to a greater extent than M1 (C2C12 control medium), possibly due to the reduced serum (20% in M1, 10% in M2). Following this, M1 was chosen as a proliferation medium for subsequent medium composition and co-culture experiments.

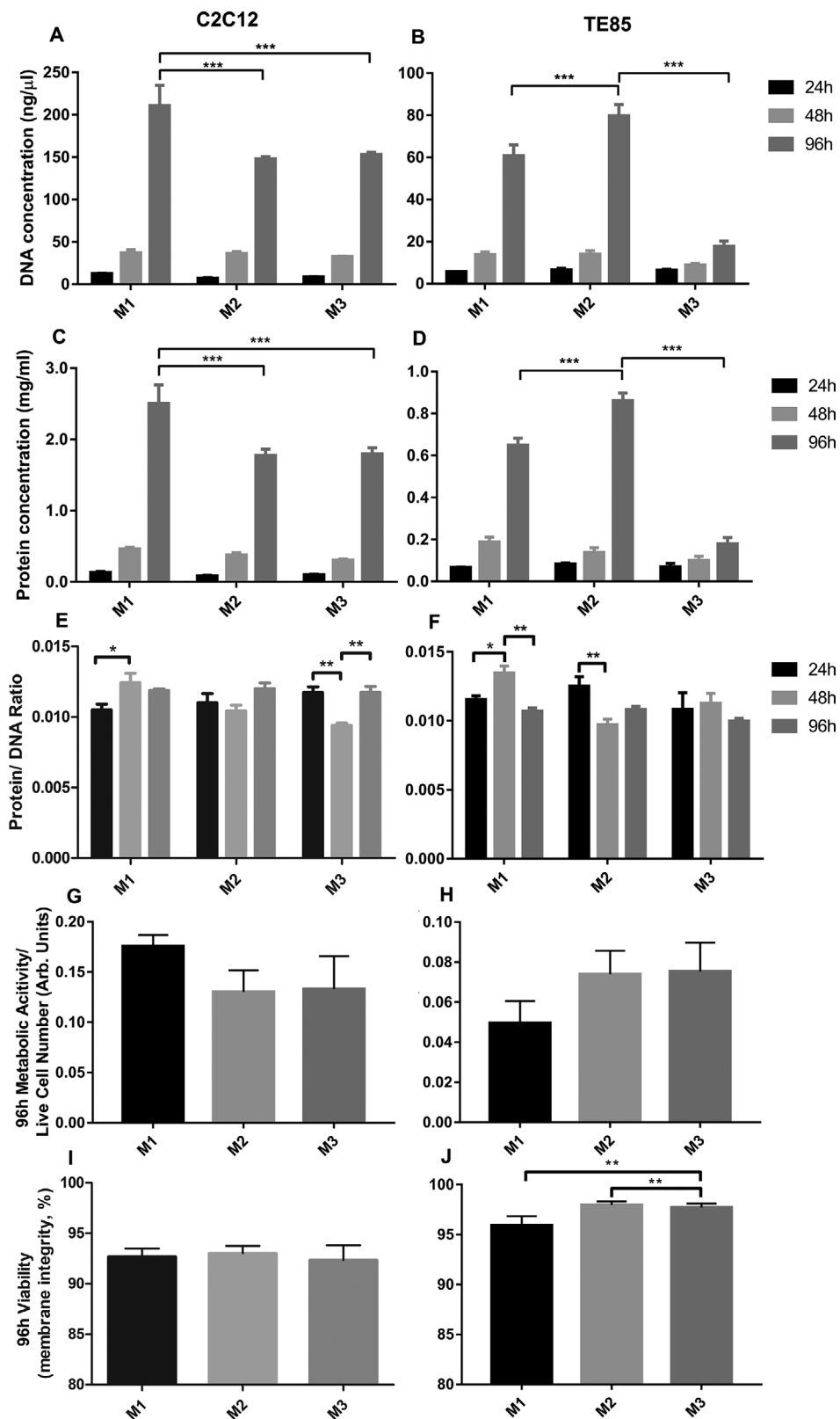


Figure 3. C2C12 and TE85 growth medium composition comparisons. DNA (A, B) and protein concentrations (C, D). E, F) Protein/DNA ratios. G, H) 96-h Metabolic activity/live cell number. I, J) 96-h Viability (membrane integrity). $n = 3$ per time point per condition + 3 replicates per well. * $p < 0.05$, ** $p < 0.01$, *** $p < 0.001$.

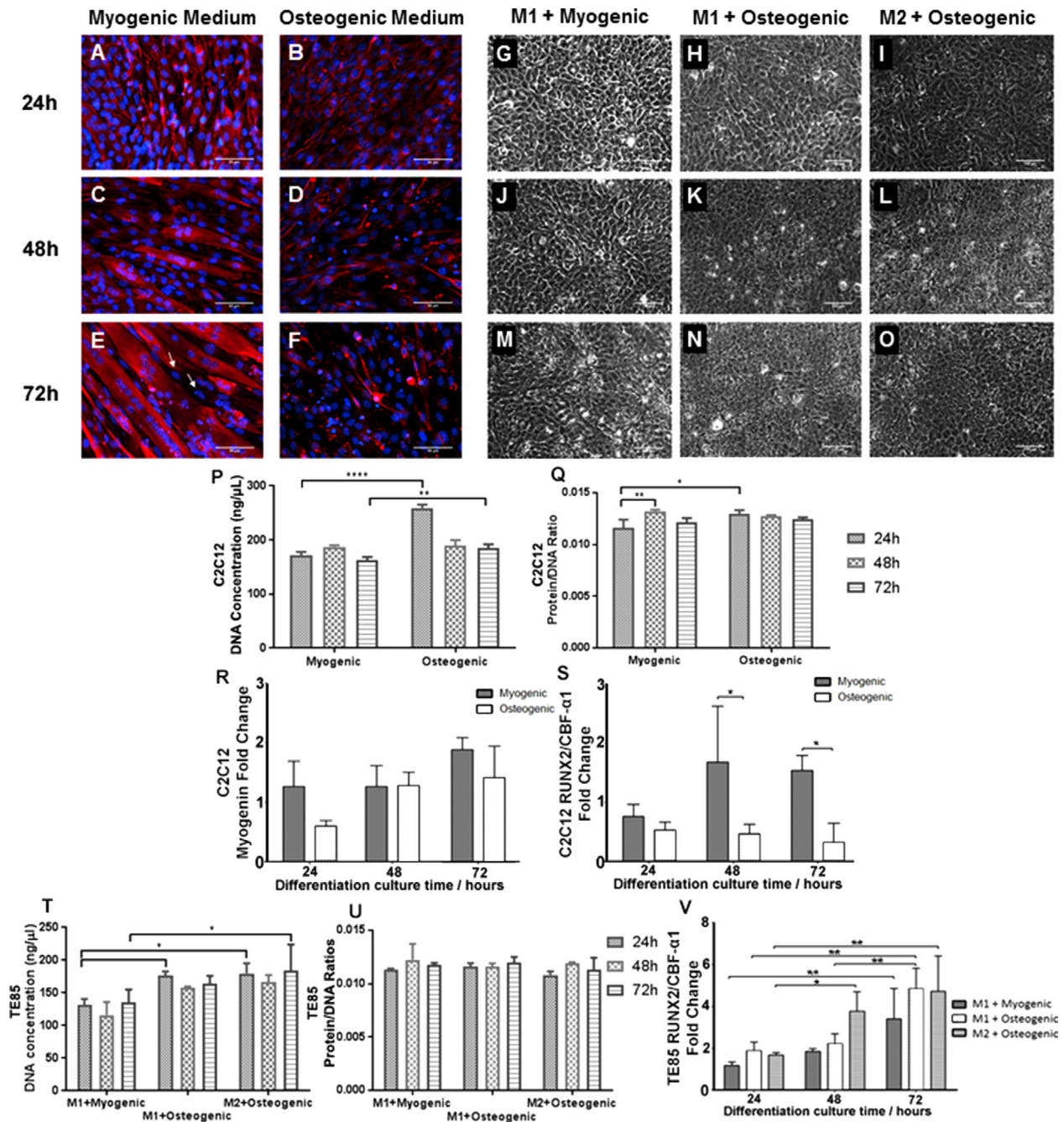


Figure 4. A–F, P–S) C2C12 and TE85 (G–O, T–V) differentiation medium composition comparisons. A–F) Monolayer C2C12 morphological observation: desmin (red) and DAPI (blue). Unfused nuclei show little or no presence of desmin (denoted by \rightarrow). G–O) Brightfield images of TE85 human osteosarcoma cells after culture to confluency in M1 and then exposure to either myogenic or osteogenic medium (M2 + osteogenic medium control). P) DNA concentrations in C2C12 cultures. Q) Protein/DNA ratios. Real-time qRT-PCR ($2^{-\Delta\Delta CT}$) profiles of myogenic and osteogenic markers. R) Myogenin expression and (S) RUNX2/CBF- α 1 expression of C2C12 cells in myogenic and osteogenic medium. TE85 culture's after 3 days (T) DNA concentrations and (U) protein/DNA ratios. V) RUNX2/CBF- α 1 expression of TE85 cultures in myogenic and osteogenic. Scale bar = 50 μ m; n = 3 culture replicates + 3 repeat measures for all conditions. * p < 0.05, ** p < 0.01, *** p < 0.001, **** p < 0.0001.

3.1.2. Differentiation Phase

Fluorescent microscopy shows C2C12s cultured in MM have successfully formed myotubes and become increasingly hypertrophic at 72 h, with some unassociated nuclei present

(Figure 4A–F). Corresponding DNA concentrations did not significantly change over the 72-h differentiation period, indicating exit from the cell cycle. This is accompanied by a significant (p < 0.01) increase in protein/DNA ratios after 48 h (Figure 4P,Q). C2C12s in osteogenic medium (OM) experienced a significant

reduction ($p < 0.0001$) in DNA concentrations after 48 h. This was without an accompanying change in protein/DNA ratios, indicating a loss in cell number, possibly due to detachment through overconfluence. However, these cultures still had greater DNA concentrations than C2C12s (MM) after 72 h. C2C12s in OM also experienced a reduction in desmin presence over the culture period, indicating a probable loss of myogenic potential.

TE85 cultures in OM show a greater concentration ($p < 0.05$) of DNA after 24 h in comparison to MM, although only M2+OM (TE85 control medium) had significantly greater DNA after 72 h ($p < 0.05$). Brightfield micrographs support this with an observable increase in cell density over time in OM cultures (Figure 4H–N and I–O) without cell size changes occurring (due to potentially harmful factors such as aging) as indicated by protein/DNA ratios not varying significantly over time (Figure 4T–U).

qRT-PCR results of C2C12 myogenin expression (Figure 4R) showed an increase over 72 h in MM, with no changes evident within OM. To confirm no osteogenic effects within the C2C12 population, RUNX2 expression was also assessed (Figure 4S) and no significant changes were observed. RUNX2 expression within TE85 cultures increased significantly in all cultures (Figure 4V). Fluorescent imaging in TE85 cultures showed no desmin presence across all cultures indicating no lineage altering effects of MM (Figure S2, Supporting Information).

With a reduction in desmin presence and no myogenic fusion, in addition to the lack of change in myogenin expression in C2C12 OM cultures as well as an increase in RUNX2 in TE85 MM cultures, M1 followed by MM has demonstrated a suitability to enable the development of a skeletal muscle and bone co-culture system.

3.2. Effects of Indirect Contact of Skeletal Muscle and Bone in Monolayer Cultures

As a monolayer representation of 3D skeletal muscle and bone cultures, monolayer cultures of C2C12 and TE85/HA were co-cultured in the same well but separated by a PDMS boundary. This was to understand the effects of TE85 and C2C12 intercellular interactions, such as paracrine signaling, and contact with HA.

Unlike the C2C12 fusion to form myotubes, TE85s do not visibly differentiate. To differentiate, cells must first exit the cell cycle, so to assess changes in TE85 cell growth, DNA concentrations were measured after direct/no exposure to HA and with/without C2C12s cultured in the adjacent chamber. TE85s co-cultured with C2C12s in the absence of HA had significantly greater DNA concentrations than all other conditions (Figure 5A). This indicates that the addition of secreted factors from the C2C12s is influencing the growth of the TE85s in co-culture. These factors would not be present in TE85 only cultures and the influence may be reduced by the presence of HA in the TE85/C2C12 + HA cultures. ALP concentrations of TE85 cultures normalized to DNA (Figure 5B) shows that the addition of C2C12 and HA does not inhibit production of ALP relative to TE85 only controls and is significantly greater ($p \leq 0.05$) than C2C12/TE85 – HA cultures.

Immunofluorescence of C2C12 cultures (Figure 5C–F) shows evidence of myogenic fusion in all cultures, although C2C12/TE85 + HA cultures appear to show reduced myotube

formation. Desmin is still present in the nonfused cells. Image analysis (Figure 5G–I) confirms that fusion is limited in C2C12s with both the presence of TE85s and HA, although not in HA conditioned medium. This suggests that TE85s paracrine and secreted factors reduce the fusion capability of C2C12s in the culture timeframe, the effect of which is enhanced with an interaction with HA.

3.3. Co-culture of TE 3D Skeletal Muscle and Bone Constructs

Prior to the creation of a musculoskeletal junction, conditions amenable to the successful co-culture of skeletal muscle and bone must first be understood. 3D skeletal muscle and bone cultures were set up and cultured in the same well. After 14 days culture (4 days M1, 10 days MM), samples were taken to analyze markers of differentiation. RUNX2/CBFA1 mRNA expression was induced nearly 150-fold ($p < 0.05$) in bone constructs co-cultured alongside engineered skeletal muscle in comparison to bone constructs cultured in isolation in the same media conditions (Figure 6A). Osteocalcin/BGLAP (Figure 6B) was also found to be more highly expressed ($p \leq 0.05$) in co-cultures. ALP concentration was not significantly different between cultures, although co-culture levels tended to be lower (Figure 6C). These results indicate that co-culture bone cell populations exhibit a greater osteogenic potential than control cultures, and also demonstrates that C2C12s positively interact with TE85 cultures in 3D. The presence of HA in the scaffold precluded the use of common stains, such as Alizarin Red, and obscures observation of the cells through brightfield microscopy, as such further analysis through microscopy could not be obtained.

Cellular fusion was observed in all constructs (Figure 6D–F), although in the co-cultured skeletal muscle construct there were large numbers of unfused cells and the existing myotubes were not as hypertrophic as those in the skeletal muscle constructs cultured in isolation. Mean maximum myotube length per image reflects this with skeletal muscle only cultures, demonstrating a significantly greater ($p \leq 0.05$) mean maximum length, although the mean length for both skeletal muscle only and co-cultures were not significantly different. However, the average number of myotubes per image was substantially reduced in co-culture constructs ($p < 0.001$). This demonstrates a continuation of the negative effects shown in monolayer cultures in the reduction during myotube formation.

4. Discussion

Successful development of a skeletal muscle and bone co-culture, which replicates key characteristics of in vivo tissue, would be of great benefit to in vitro investigations into the musculoskeletal system and could enable the progress toward the generation of a full in vitro musculoskeletal junction (muscle–tendon–bone). Progression of such a culture system with standardized manufacturing parameters, such as those proposed by Wragg,^[50,51] could also reduce the reliance on animal models in preclinical studies, while also allowing for the testing of efficacy and toxicity of developmental pharmaceuticals, biomaterials, and medical devices in a more biomimetic environment. In the present study, the

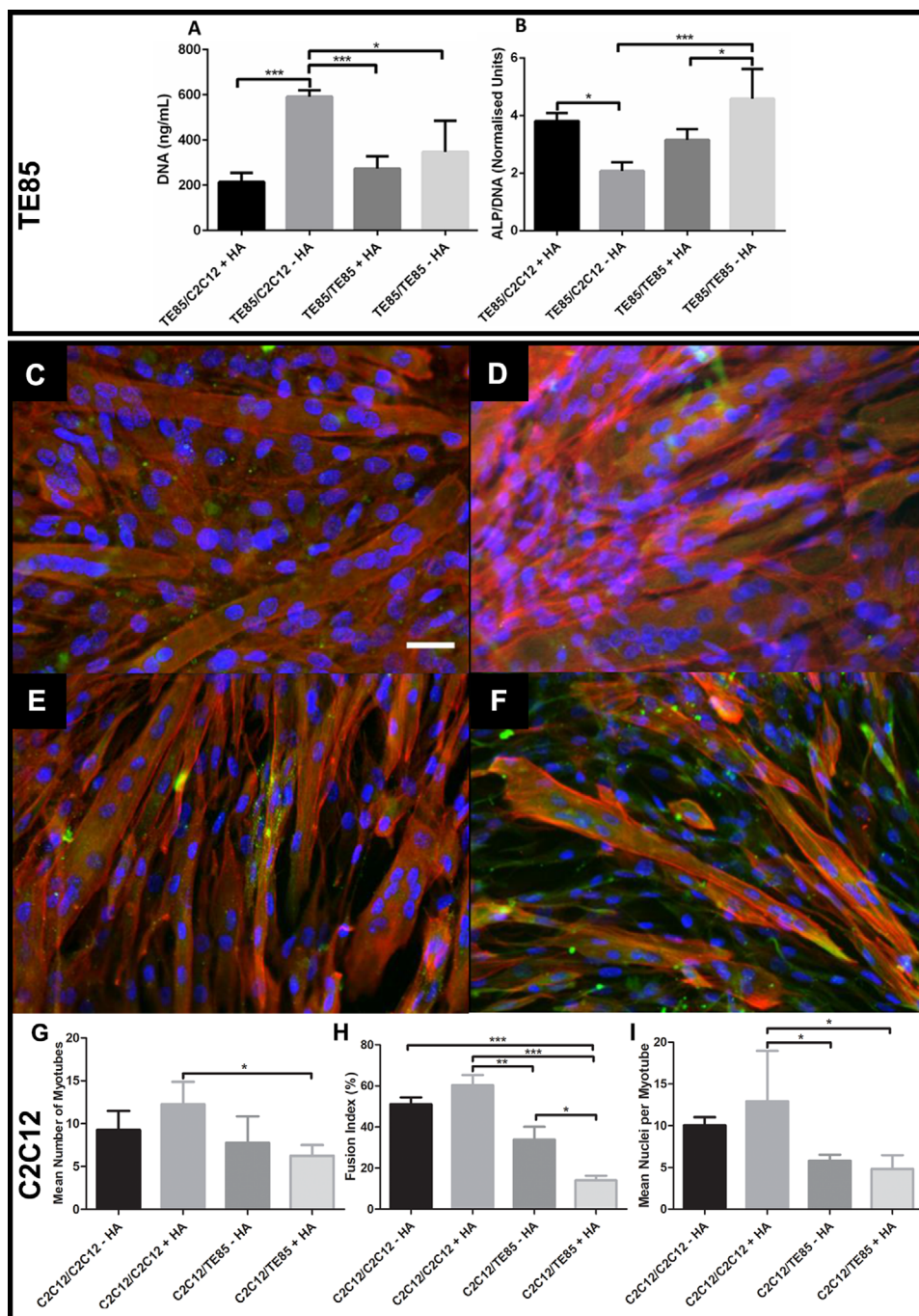


Figure 5. Monolayer co-culture differentiation: TE85 cell population DNA quantification and ALP/DNA ratio after 7 days culture (4 days in growth medium + 3 days in differentiation medium). A) DNA concentrations. B) ALP/DNA ratios. Immunofluorescent images of (C) C2C12, (D) C2C12 + HA conditioned media, (E) C2C12/TE85 - HA, and (F) C2C12/TE85 + HA. Blue = nuclei (DAPI); red = F-actin (rhodamine phalloidin); green = desmin (Chromo 488). Scale bar = 20 μ m. G) Mean number of myotubes per image. H) Fusion index per image. I) Mean nuclei per myotube per image. $n = 3$ replicate cultures + 3 repeat measures. * $p < 0.05$, ** $p < 0.01$, *** $p < 0.001$, bars represent \pm SD.

variables required to facilitate co-culture of both the C2C12 myogenic and TE85 osteogenic cell lines have been established, culminating in successful growth and differentiation of skeletal muscle and bone 3D tissues in vitro.

As one of the major factors affecting myoblast fusion and bone matrix secretion, investigating the effects of different medium

composition on proliferation and differentiation is of high importance. While co-culture systems described within the literature report the influence of one cell type on the other, these papers have yet to describe the conditions which allow for the successful culture and differentiation of both cell types in a single medium system through experimental comparisons.^[52–55]

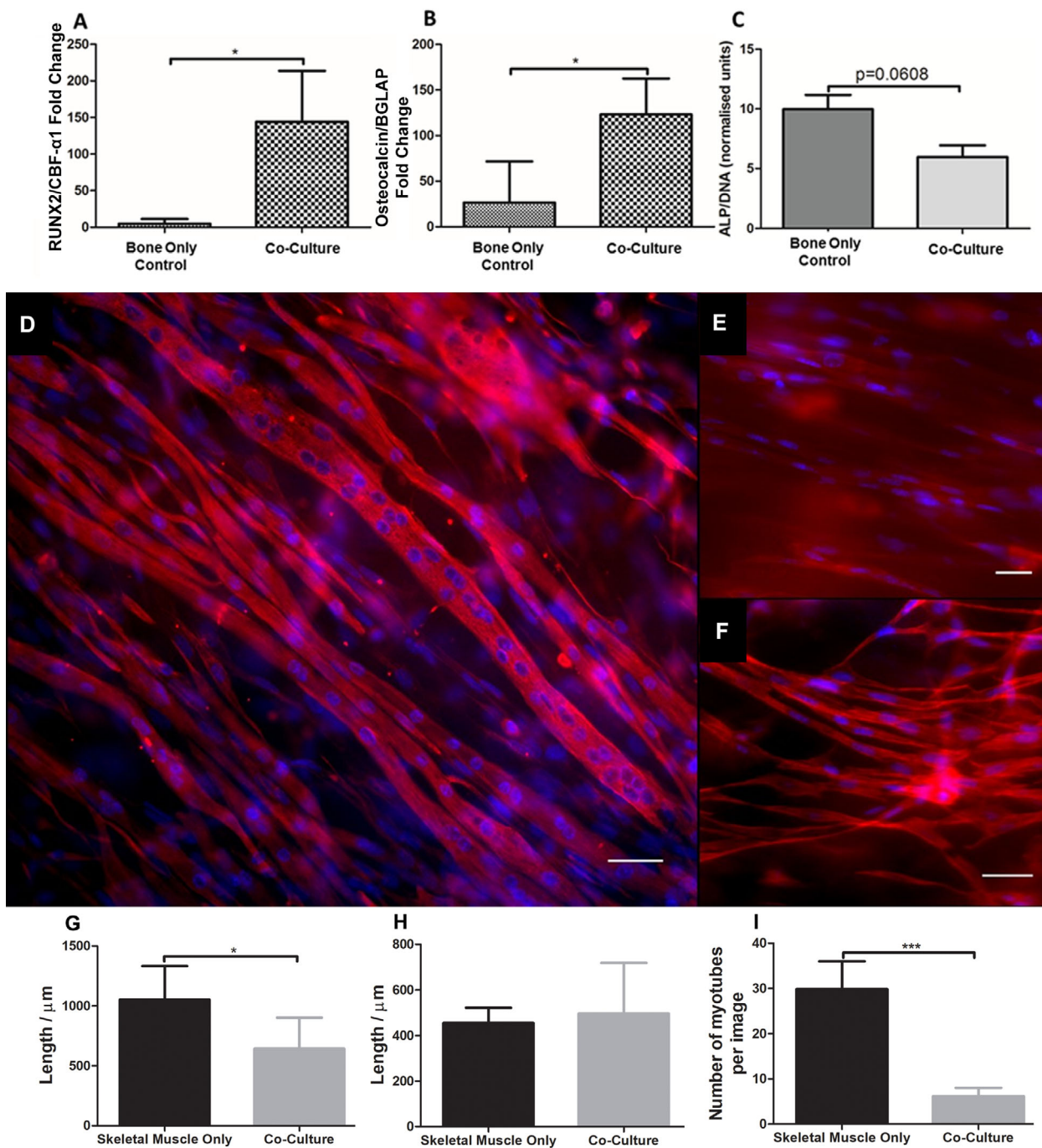


Figure 6. 3D skeletal muscle and bone co-culture: Real-time qRT-PCR ($2^{-\Delta\Delta CT}$) measurement of RUNX2/CBF- α 1 (A), osteocalcin/BGLAP (B), and ALP/DNA ratios (C) in co-culture and bone model only controls. Immunofluorescence of (D) skeletal muscle only constructs myotubes, (E) aligned myotubes within a skeletal muscle construct co-cultured with bone constructs (fluorescence interference from collagen matrix), and (F) fused and unfused C2C12s within a skeletal muscle construct co-cultured with bone constructs. Blue = nuclei; red = desmin. Scale bar = 100 μ m. Image analysis of myotube characteristics: G) Maximum myotube length. H) Mean myotube length. I) Number of myotubes per image. $n = 4$ repeat conditions + 3 repeat measures. * $p \leq 0.05$, *** $p < 0.001$, bars represent \pm SD.

In the experiments reported herein, a restriction in the concentrations of glucose between medium significantly negatively affected the C2C12 line and was not offset by the addition of glutamine.^[56–58] A deficit in the fetal bovine serum (FBS) supplement concentration was also implicated in the restriction

of population growth of the myogenic cells. Myogenic cell lineages are typically cultured in a high-glucose (4500 mg L⁻¹) basal medium with at least 10% FBS, although 20% FBS supplementation has been shown to produce more favorable results.^[59–63] Conversely, the TE85 cell line showed greater proliferation with

a lower glutamine, glucose, and FBS concentrations. Osteogenic cell lineages are typically cultured in low-glucose (1000 mg L⁻¹) medium with 10% FBS and an addition of nonessential amino acids.^[64–68] Regardless of these outcomes, both skeletal muscle and osteoblast-like cell types show a capacity for proliferation in all media with a bias toward each cell type's typical culture medium as expected. However, C2C12s were affected to a greater extent than TE85s, resulting in high-glucose DMEM + 20% FBS being chosen as a suitable proliferation medium for both cell lines.

Myogenic cells have also shown the ability to differentiate along an osteoblastic lineage and conditions promoted through blast and crush injury demonstrate this capacity *in vivo*.^[59,69–72] As a marker for osteoblast progression, RUNX2 has been established as the initial trigger of the osteogenic cascade, resulting in ALP production and an upregulation of BGLAP/osteocalcin. Under culture with common osteogenic supplements (β -glycerol-phosphate, ascorbic acid, and dexamethasone), C2C12s showed no change in myogenin expression across 3 days and no significant differences in RUNX2 expression. This is in comparison to the classic upregulation followed by subsequent decrease in myogenin expression observed in MM serum-starved cultures.^[42,73–75] Under reduced serum conditions (MM), C2C12s fused to form small myotubes dispersed between desmin positive cells, which later progressed to form multiple hypertrophic myotubes, in line with classic *in vitro* skeletal muscle culture. However, C2C12s cultured in OM demonstrated a decrease in desmin presence with an increase in nondesmin-associated nuclei and punctate staining. The low-glucose aspect of the OM potentially caused a reduction in metabolic activity, accompanied by the presence of dexamethasone, a known inducer of atrophy^[76–78] and other osteogenic factors may have caused a reversion to a more progenitor-like state, alluded to in skeletal muscle calcification conditions.^[69] A lack of RUNX2/Cbfa1 upregulation supports a reversion theory to a less committed cell type, rather than a direct lineage change as in the case of BMP-2 stimulated culture.^[59]

Much like the skeletal MPCs, osteoblasts exit the cell cycle prior to differentiating.^[79,80] Once the TE85 cultures growth profiles are stabilized, they displayed an upregulation of RUNX2/Cbfa1 in all cultures after 3 days and nondesmin-associated nuclei without evidence of cellular fusion. The concentration and the type of serum in the differentiation medium do not seem to affect the final expression of RUNX2/CBFA1. However, the osteogenic supplements may reduce the latent time before expression is upregulated. Therefore, low non-fetal serum (2% horse serum) could be used in subsequent studies involving osteoblasts-like cells, which would reduce the costs involved in cultures of this type.

Once defining the appropriate medium compatibility protocol, the influence of each cell type in the same culture environment was assessed with the addition of HA to stimulate further differentiation and mimic part of the composition of *in vivo* bone matrix. HA, in this case, was found to inhibit DNA concentrations within TE85 populations in co-culture with C2C12s but increase ALP/DNA in TE85 only and co-culture conditions. TE85s may have downregulated markers relevant to the production of ALP and are therefore self-regulating responses once exposed to HA. This self-regulation has been reported in reference to organic/inorganic pyrophosphate ratios.^[81]

Current monolayer toxicity tests are generally single cell type and conducted in accordance with ISO10993 for medicinal devices or through high-throughput studies in drug discovery (ISO Identification of Medicinal Products). The monolayer system presented here, using both skeletal muscle and osteoblast cell lines, and incorporating elements of ECM to induce osteogenesis, creates a more relevant system for testing neighborhood effects of toxicity. The ease of setup would lend itself to high-throughput techniques in smaller culture wells, although alternatives such as trans-well inserts should be considered.^[82–85] Additionally, this system could be used to investigate musculoskeletal conditions, such as the exposure of skeletal muscle to bone cells and ECM in blast injuries^[69] by removal of the central barrier, similar to Wang et al.,^[86] in which mature populations were allowed to migrate and mix when observing enthesis healing.

The final component of the 3D co-culture, the collagen scaffold, allows the cells to reside in three dimensions. Reported medium protocols do not normally change between monolayer and 3D work, however, 3D cultures exhibit longer culture periods before definitive differentiation.^[16,23,87] Additionally, considering the different volumetric shapes and mechanical influences (anchor points) to which each of the skeletal muscle and bone construct were developed, a novel co-culture system needed to be created to allow co-exposure to the medium. Previous co-culture systems utilized a well-established delamination model, creating cylindrical 3D constructs and concentrating on biological outputs without regard to creating individual properties to best support each tissues formation.^[88–90] The platform developed here sought to enable the formation of each of the constructs as previously described, in both shape and cellular differentiation.^[5,11,16,50] Subsequent observation of each construct did not demonstrate any obvious deviation from single construct formation and analysis of differentiation showed enhancement of gene expression in the bone construct. While fusion in the skeletal muscle constructs was diminished, an increased culture period may encourage similar myotube characteristics to isolated skeletal muscle constructs. This diminished myotube fusion in the presence of HA and TE85s was also observed in the monolayer co-cultures and indicates continuity in cell behavior between monolayer and 3D platforms. Increasing bone-specific gene expression in the presence of skeletal muscle, without mechanical loading, is supported by a growing body of work in the influence of “myokines” on bone formation.^[91–93] The effect of bone on muscle has had little study, although it has been reported that bone cell culture secretions impair skeletal muscle formation.^[94]

Considering the reported successes in skeletal muscle–tendon and bone–tendon models,^[88,90] as well as tendon formation in a collagen hydrogel, the addition of a tendon component to this model should not be considered a prohibitive obstacle to the construction of an *in vitro* musculoskeletal junction.^[95,96] Ultimately, this strategy can be applied to more physiologically relevant human stem cell–derived cell types involved in the native musculoskeletal junction in order to achieve a more accurate prediction of drug testing responses.

In summary, this study represents the first reported instance of simultaneous 3D TE skeletal muscle and bone differentiation in co-culture, with evidence of an enhancing effect on bone-specific gene expression. A single GM (high-glucose DMEM + 20% FBS) was found to enable proliferation of the C2C12

muscle precursor and the TE85 osteosarcoma cell lines. This was coupled with high-glucose DMEM + 2% horse serum to enable fusion of C2C12s to form myotubes, an increase in expression of RUNX2/CBFA1 in TE85 cultures. When in monolayer co-culture, both cell types could proliferate and differentiate in the presence of each other and HA with the chosen medium protocol. 3D co-culture of skeletal muscle and bone in vitro demonstrated enhanced osteogenic gene expression in the bone model, in comparison to isolated bone controls, with no significant differences in ALP activity. Co-cultured skeletal muscle constructs retained a capacity for myoblast fusion, although this appeared diminished when compared to controls.

Future work should seek to use the methods described here to create a 3D tendon construct with a view to attachment to the bone and skeletal muscle models to form a full in vitro 3D TE musculoskeletal junction (muscle–tendon–bone). Additionally, the monolayer co-culture model should be further characterized in conjunction with the 3D co-culture to enable a comparative platform progression for testing.

Supporting Information

Supporting Information is available from the Wiley Online Library or from the author.

Acknowledgement

Funding from the Doctoral Training Centre of Regenerative Medicine (EPSRC, UK) is gratefully acknowledged.

Conflict of Interest

The authors declare no conflict of interest.

Keywords

bone, co-culture, medium compatibility, skeletal muscle, tissue engineering

Received: March 25, 2019

Revised: July 5, 2019

Published online:

- [1] K.-H. Nam, A. S. T. Smith, S. Lone, S. Kwon, D.-H. Kim, *J. Lab. Autom.* **2015**, *20*, 201.
- [2] H. Vandenburg, J. Shansky, F. Benesch-Lee, V. Barbata, J. Reid, L. Thorrez, R. Valentini, G. Crawford, *Muscle Nerve* **2008**, *37*, 438.
- [3] T. Eschenhagen, W. H. Zimmermann, *Circ. Res.* **2005**, *97*, 1220.
- [4] K. S. Smalley, M. Lioni, K. Noma, N. K. Haass, M. Herlyn, *Expert Opin. Drug Discovery* **2008**, *3*, 1.
- [5] A. S. T. Smith, S. Passey, L. Greensmith, V. Mudera, M. P. Lewis, *J. Cell. Biochem.* **2012**, *113*, 1044.
- [6] H. J. Mulhall, M. P. Hughes, B. Kazmi, M. P. Lewis, F. H. Labeed, *Biochim. Biophys. Acta, Gen. Subj.* **2013**, *1830*, 5136.
- [7] A. Mobasheri, M. Lewis, in *Regenerative Medicine and Tissue Engineering* (Ed: J. A. Andrades), InTech, Rijeka, Croatia **2013**, pp. 509–541.
- [8] G. Langley, *RSDA* **2009**, *1*, 161.
- [9] N. T. Elliott, F. Yuan, *J. Pharm. Sci.* **2011**, *100*, 59.
- [10] M. Juhas, G. C. Engelmayr, A. N. Fontanella, G. M. Palmer, N. Bursac, *Proc. Natl. Acad. Sci. USA* **2014**, *111*, 5508.
- [11] A. P. Sharples, D. J. Player, N. R. W. Martin, V. Mudera, C. E. Stewart, M. P. Lewis, *Aging Cell* **2012**, *11*, 986.
- [12] S. Sundelacruz, C. Li, Y. J. Choi, M. Levin, D. L. Kaplan, *Biomaterials* **2013**, *34*, 6695.
- [13] S. H. Choi, K. Y. Chung, B. J. Johnson, G. W. Go, K. H. Kim, C. W. Choi, S. B. Smith, *J. Nutr. Biochem.* **2013**, *24*, 539.
- [14] H. Fujita, A. Endo, K. Shimizu, E. Nagamori, *Biotechnol. Bioeng.* **2010**, *107*, 894.
- [15] S. Hinds, N. Tyhovich, C. Sistrunk, L. Terracio, *Sci. World J.* **2013**, *2013*, 1.
- [16] D. J. Player, N. R. W. Martin, S. L. Passey, A. P. Sharples, V. Mudera, M. P. Lewis, *Biotechnol. Lett.* **2014**, *36*, 1113.
- [17] N. R. W. Martin, M. C. Turner, R. Farrington, D. J. Player, M. P. Lewis, *J. Cell. Physiol.* **2017**, *232*, 2788.
- [18] Y. Huang, R. G. Dennis, L. Larkin, K. Baar, *J. Appl. Physiol.* **2005**, *98*, 706.
- [19] C. Neidlinger-Wilke, E. S. Grood, J. H.-C. Wang, R. A. Brand, L. Claes, *J. Orthop. Res.* **2001**, *19*, 286.
- [20] R. G. Dennis, P. E. Kosnik, *In Vitro Cell. Dev. Biol. – Anim.* **2000**, *36*, 327.
- [21] C. A. Powell, B. L. Smiley, J. Mills, H. H. Vandenburg, *Am. J. Physiol.: Cell Physiol.* **2002**, *283*, C1557.
- [22] V. Mudera, A. S. T. Smith, M. A. Brady, M. P. Lewis, *J. Cell. Physiol.* **2010**, *225*, 646.
- [23] N. R. W. Martin, S. L. Passey, D. J. Player, A. Khodabakus, R. A. Ferguson, A. P. Sharples, V. Mudera, K. Baar, M. P. Lewis, *Biomaterials* **2013**, *34*, 5759.
- [24] K. J. M. Boonen, M. L. P. Langelaan, R. B. Polak, D. W. J. van der Schaft, F. P. T. Baaijens, M. J. Post, *J. Biomech.* **2010**, *43*, 1514.
- [25] S. Hinds, W. Bian, R. G. Dennis, N. Bursac, *Biomaterials* **2011**, *32*, 3575.
- [26] M. Eastwood, V. C. Mudera, D. A. Mcgrouter, R. A. Brown, *Cell Motil. Cytoskeleton* **1998**, *40*, 13.
- [27] C. T. Laurencin, A. M. Ambrosio, M. D. Borden, J. A. Cooper, *Annu. Rev. Biomed. Eng.* **1999**, *1*, 19.
- [28] J. L. Brown, S. G. Kumbar, C. T. Laurencin, *Bone Tissue Engineering*, Elsevier, Amsterdam, The Netherlands **2013**.
- [29] F. N. Syed-Picard, L. M. Larkin, C. M. Shaw, E. M. Arruda, *Tissue Eng., Part A* **2009**, *15*, 187.
- [30] M. S. Kamath, S. S. S. J. Ahmed, M. Dhanasekaran, S. W. Santosh, *Int. J. Nanomed.* **2014**, *9*, 183.
- [31] C. W. Cheng, L. D. Solorio, E. Alsberg, *Biotechnol. Adv.* **2014**, *32*, 462.
- [32] H. Petite, V. Viateau, W. Bensaïd, A. Meunier, C. de Pollak, M. Bourguignon, K. Oudina, L. Sedel, G. Guillemin, *Nat. Biotechnol.* **2000**, *18*, 959.
- [33] A. L. Boskey, *Natural and Synthetic Hydroxyapatites*, Elsevier, Amsterdam, The Netherlands **2013**.
- [34] L. L. Hench, S. M. Best, *Ceramics, Glasses, and Glass-Ceramics*, Elsevier, Amsterdam, The Netherlands **2013**.
- [35] P. Gentile, V. Chiono, I. Carmagnola, P. V. Hatton, *Int. J. Mol. Sci.* **2014**, *15*, 3640.
- [36] T. Lou, X. Wang, G. Song, *J. Mater. Sci.: Mater. Med.* **2015**, *26*, 34.
- [37] S. K. Padmanabhan, A. Sannino, A. Licciulli, *Key Eng. Mater.* **2014**, *587*, 239.
- [38] R. Murugan, S. Ramakrishna, *Tissue Eng.* **2006**, *12*, 435.
- [39] Y. B. Kim, G. H. Kim, *ACS Comb. Sci.* **2015**, *17*, 87.
- [40] F. Henson, A. Getgood, *Open Orthop J* **2011**, *5*, 261.
- [41] A. Oryan, S. Alidadi, A. Moshiri, N. Maffulli, *J. Orthop. Surg. Res.* **2014**, *9*, 18.
- [42] F. Langenbach, J. Handschel, *Stem Cell Res. Ther.* **2013**, *4*, 117.

- [43] I. Wimpenny, K. Hampson, Y. Yang, N. Ashammakhi, N. R. Forsyth, *Tissue Eng., Part C* **2010**, *16*, 503.
- [44] N. Bölgen, Y. Yang, P. Korkusuz, E. Güzel, A. J. El Haj, E. Pişkin, *Tissue Eng., Part A* **2008**, *14*, 1743.
- [45] C. Heinemann, S. Heinemann, H. Worch, T. Hanke, *Eur. Cells Mater.* **2011**, *21*, 80.
- [46] H. Cheng, W. Jiang, F. M. Phillips, R. C. Haydon, Y. Peng, L. Zhou, H. H. Luu, N. An, B. Breyer, P. Vanichakarn, J. P. Szatkowski, J. Y. Park, T. C. He, *J. Bone Joint SurgAm* **2003**, *85*, 1544.
- [47] Y. Liu, D. J. Williams, *IEEE Trans. NanoBiosci.* **2010**, *9*, 1.
- [48] K. J. Livak, T. D. Schmittgen, *Methods* **2001**, *25*, 402.
- [49] P. Desjardins, J. B. Hansen, M. Allen, *J. Vis. Exp.* **2009**. <https://doi.org/10.3791/1610>.
- [50] N. M. Wragg, Thesis, Loughborough University (Loughborough, UK) **2016**.
- [51] N. M. Wragg, D. J. Player, N. R. W. Martin, Y. Liu, M. P. Lewis, *Biotechnol. Bioeng.* **2019**, *116*, 2364.
- [52] A. G. Mikos, S. W. Herring, P. Ochareon, J. Elisseeff, H. H. Lu, R. Kandel, F. J. Schoen, M. Toner, D. Mooney, A. Atala, M. E. Van Dyke, D. Kaplan, G. Vunjak-Novakovic, *Tissue Eng.* **2006**, *12*, 3307.
- [53] V.-S. Eckle, B. Drexler, C. Grasshoff, T. Seeger, H. Thiermann, B. Antkowiak, *ALTEX* **2014**, *31*, 433.
- [54] M. Kino-oka, J. Kim, K. Kurisaka, M.-H. Kim, *J. Biosci. Bioeng.* **2013**, *115*, 96.
- [55] A. Kulesza, A. Burdzinska, I. Szczepanska, W. Zarychta-Wisniewska, B. Pajak, K. Bojarczuk, B. Dybowski, L. Paczek, *PLoS One* **2016**, *11*, e0161693.
- [56] A. Behjouciar, C. Kontoravdi, K. M. Polizzi, *PLoS One* **2012**, *7*, e34512.
- [57] F. Lu, P. C. Toh, I. Burnett, F. Li, T. Hudson, A. Amanullah, J. Li, *Biotechnol. Bioeng.* **2013**, *110*, 191.
- [58] M. Yuneva, N. Zamboni, P. Oefner, R. Sachidanandam, Y. Lazebnik, *J. Cell Biol.* **2007**, *178*, 93.
- [59] T. Katagiri, A. Yamaguchi, M. Komaki, E. Abe, N. Takahashi, T. Ikeda, V. Rosen, J. M. Wozney, A. Fujisawa-Sehara, T. Suda, *J. Cell Biol.* **1994**, *127*, 1755.
- [60] S. T. Cooper, A. L. Maxwell, E. Kizana, M. Ghodusi, E. C. Hardeman, I. E. Alexander, D. G. Allen, K. N. North, *Cell Motil. Cytoskeleton* **2004**, *58*, 200.
- [61] H. Park, R. Bhatta, R. Saigal, M. Radisic, N. Watson, R. Langer, G. Vunjak-Novakovic, *J. Tissue Eng. Regener. Med.* **2008**, *2*, 279.
- [62] M. Costantini, S. Testa, P. Mozetic, A. Barbetta, C. Fuoco, E. Fornetti, F. Tamiro, S. Bernardini, J. Jaroszewicz, W. Świążkowski, M. Trombetta, L. Castagnoli, D. Seliktar, P. Garstecki, G. Cesareni, S. Cannata, A. Rainer, C. Gargioli, *Biomaterials* **2017**, *131*, 98.
- [63] S. B. Sharp, M. Lee, E. Enriquez, A. Ghebremedhin, P. Momjian, S. Kim, L. Sunday, M. Villalvazo, L. S. Carvajal, S. Avari, *In Vitro Cell Dev Biol – Anim* **1995**, *31*, 749.
- [64] I. A. San Martin, N. Varela, M. Gaete, K. Villegas, M. Osorio, J. C. Tapia, M. Antonelli, E. E. Mancilla, B. P. Pereira, S. S. Nathan, J. B. Lian, J. L. Stein, G. S. Stein, A. J. van Wijnen, M. Galindo, *J. Cell. Physiol.* **2009**, *221*, 560.
- [65] J. Struewer, P. P. Roessler, K. F. Schuettler, V. Ruppert, T. Stein, N. Timmesfeld, J. R. Paletta, T. Efe, *Int. Orthop.* **2014**, *38*, 1083.
- [66] G. L. Jones, R. Walton, J. Czernuszka, S. L. Griffiths, A. J. El Haj, S. H. Cartmell, *J. Biomed. Mater. Res., Part A* **2010**, *94*, 1244.
- [67] M. E. Gomes, R. L. Reis, A. M. Cunha, C. A. Blitterswijk, J. D. de Bruijn, *Biomaterials* **2001**, *22*, 1911.
- [68] Z. Wang, Y. Ma, J. Wei, X. Chen, L. Cao, W. Weng, Q. Li, H. Guo, J. Su, *Sci. Rep.* **2017**, *7*, 823.
- [69] O. G. Davies, L. M. Grover, N. Eisenstein, M. P. Lewis, Y. Liu, *Calcif. Tissue Int.* **2015**, *97*, 432.
- [70] A. C. M. Sinanan, P. G. Buxton, M. P. Lewis, *Biol. Cell* **2006**, *98*, 203.
- [71] H. Mulhalla, M. Patel, K. Alqahtani, C. Mason, M. P. Lewis, I. Wall, *J. Tissue Eng. Regener. Med.* **2011**, *5*, 629.
- [72] J. D. Starkey, M. Yamamoto, S. Yamamoto, D. J. Goldhamer, *J. Histochem. Cytochem.* **2011**, *59*, 33.
- [73] N. Maffulli, W.B. Leadbetter, P. Renström, *Tendon Injuries : Basic Science and Clinical Medicine*, Springer, London **2005**.
- [74] N. Maegawa, K. Kawamura, M. Hirose, H. Yajjima, Y. Takakura, H. Ohgushi, *J. Tissue Eng. Regener. Med.* **2007**, *1*, 306.
- [75] C. B. Khatiwala, P. D. Kim, S. R. Peyton, A. J. Putnam, *J. Bone Miner. Res.* **2009**, *24*, 886.
- [76] J. Qin, R. Du, Y.-Q. Yang, H.-Q. Zhang, Q. Li, L. Liu, H. Guan, J. Hou, X. R. An, *Res. Vet. Sci.* **2013**, *94*, 84.
- [77] A. A. L. O. Krug, A. G. Macedo, A. S. Zago, *Muscle Nerve* **2012**, *53*, 779.
- [78] M. D. Girón, J. D. Vilchez, S. Shreeram, R. Salto, M. Manzano, E. Cabrera, N. Campos, N. K. Edens, R. Rueda, J. M. López-Pedrosa, *PLoS One* **2015**, *10*, e0117520.
- [79] N. Funato, K. Ohtani, K. Ohyama, T. Kuroda, M. Nakamura, *Mol. Cell. Biol.* **2001**, *21*, 7416.
- [80] T. Gaur, C. J. Lengner, H. Hovhannisyann, R. A. Bhat, P. V. N. Bodine, B. S. Komm, A. Javed, A. J. van Wijnen, J. L. Stein, G. S. Stein, J. B. Lian, *J. Biol. Chem.* **2005**, *280*, 33132.
- [81] E. E. Golub, G. Harrison, A. G. Taylor, S. Camper, I. M. Shapiro, *Bone Miner.* **1992**, *17*, 273.
- [82] Y. Takegahara, K. Yamanouchi, K. Nakamura, S. Nakano, M. Nishihara, *Exp. Cell Res.* **2014**, *324*, 105.
- [83] J. S. Dines, D. A. Grande, D. M. Dines, *J. Shoulder Elbow Surg.* **2007**, *16*, S204.
- [84] Y. Miki, K. Ono, S. Hata, T. Suzuki, H. Kumamoto, H. Sasano, *J. Steroid Biochem. Mol. Biol.* **2012**, *131*, 68.
- [85] G. Im, *Tissue Eng., Part B* **2014**, *00*, 1.
- [86] I.-N. E. Wang, J. Shan, R. Choi, S. Oh, C. K. Kepler, F. H. Chen, H. H. Lu, *J. Orthop. Res.* **2007**, *25*, 1609.
- [87] S. Burattini, P. Ferri, M. Battistelli, R. Curci, F. Luchetti, E. Falcieri, *Eur. J. Histochem.* **2004**, *48*, 223.
- [88] J. Ma, K. Goble, M. Smietana, T. Kostrominova, L. Larkin, E. M. Arruda, *J. Biomech. Eng.* **2009**, *131*, 101017.
- [89] L. M. Larkin, S. Calve, T. Y. Kostrominova, E. M. Arruda, *Tissue Eng.* **2006**, *12*, 3149.
- [90] T. Y. Kostrominova, S. Calve, E. M. Arruda, L. M. Larkin, *Histol. Histopathol.* **2009**, *24*, 541.
- [91] K. Shah, Z. Majeed, J. Jonason, R. J. O'Keefe, *Curr. Osteoporos. Rep.* **2013**, *11*, 130.
- [92] L. A. Riley, K. A. Esser, *Curr. Osteoporos. Rep.* *15*, **2017**, 222.
- [93] B. Guo, Z. K. Zhang, C. Liang, J. Li, J. Liu, A. Lu, B. T. Zhang, G. Zhang, *Calcif. Tissue Int.* **2017**, *100*, 184.
- [94] C. L. Wood, P. D. Pajevic, J. H. Gooi, *Bone Reports* **2017**, *6*, 74.
- [95] J. Garvin, J. Qi, M. Maloney, A. J. Baner, *Tissue Eng.* **2003**, *9*, 967.
- [96] P. Sawadkar, S. Alexander, M. Tolc, J. Wong, D. McGrouther, L. Bozec, V. Muderu, *BioRes. Open Access* **2013**, *2*, 327.